The Use of Texture Measures in Improving Mine Classification Performance

Martin G. Bello, Alphatech Inc. Gerald J. Dobeck,
NSWC Coastal Systems Station

6 New England Executive Park
Burlington, MA. 01803, USA
marty.bello@alphatech.com

Abstract- Research over the last 9 years has resulted in an effective mine classification approach that involves the use of image-segmentation based screening methods followed by multilayer perceptron networks for mine classification. The present approach centers around a baseline 23 Feature set related to highlight, shadow, and highlight/shadow contrast statistic based segmentations, and the use of associated statistical and shape related factors. In the work described here we investigate the improvement of baseline performance by incorporating image texture related features such as Cooccurrence Matrix related factors.

I. INTRODUCTION

The need for automated processing in the detection/classification of mines to reduce the workload of human sonar operators is clear. The mine-detection/classification system described here is partitioned into an anomaly screening stage, followed by a classification stage involving the calculation of features on blobs, and their input into a multilayer perceptron neural network.

In order to obtain sufficiently low false alarm densities for an actual system, several strategies can be employed. Multiple mine hunting algorithms may be fused, i.e. detections/classifications may be effectively combined by imposing the constraint that a given mine like blob derived from one algorithm must intersect at least one blob obtained from each of an aggregate collection of distinct algorithms. This strategy is currently employed by the Naval Coastal Systems Station (CSS) in combining the results obtained from the CSS, Alphatech, Raytheon, and Lockheed-Martin mine hunting algorithms.

To improve the performance of individual Mine Classification algorithms, new feature sets are continually under investigation, particularly as the resolution and quality of available side-scan sonar data improves.
In the discussion that follows section 2.0 defines the overall mine detection/classification(CAD/CAC) algorithm structure. Defining our CAD/CAC algorithm will involve defining the formation of our “Baseline”, 23 dimensional feature set, and additional features considered here for augmenting the Baseline set, consisting of Haralick’s Cooccurrence Matrix derived factors[1].

In section 3.0 classification performance results obtained from fusing classifiers based on the baseline and texture features, respectively, are compared with baseline performance. Finally, in section 5.0 conclusions are made.

II. MINE HUNTING ALGORITHM STRUCTURE

The structure of the aggregate detection/classification algorithm studied here is summarized in Fig. 1. The image normalization algorithm[2] in Fig. 1 was developed by Dr.Gerald Dobeck of the NSWC CSS(Naval Surface Warfare Center Coastal System Station), as well as others, and consists in the use of a combined forward/backward low-pass filtering approach to estimate local background intensity at each pixel along a range profile. The input image intensity along the range profile is then normalized by those local background intensity estimates. This results in more homogeneous background characteristics, making highlights and shadows more uniformly visible. The purpose of the anomaly-screening algorithm is to extract blobs; i.e. collections of connected pixels, which correspond to candidate mine-like (ML) objects. These candidate ML blobs will be referred to as image Tokens. A vector of classification features, to be defined in the discussion that follows, is then calculated for each image Token. A trained multilayer perceptron network is then employed, using the Token classification feature vectors as inputs, in order to obtain “target” and “clutter” output statistics, which may be viewed as approximate posterior probabilities. The logarithm of the ratio of “target” over “clutter” output node statistics is calculated and corresponds to a log-likelihood ratio statistic- LLR. These LLR values are ranked and thresholded to determine a final output ML Token list.

Report Documentation Page

Form Approved
OMB No. 0704-0188

1. REPORT DATE	2. REPORT TYPE	3. DATES COVERED
01 SEP 2003	**N/A**	**-**

4. TITLE AND SUBTITLE	5a. CONTRACT NUMBER
The Use of Texture Measures in Improving Mine Classification Performance	5b. GRANT NUMBER
	5c. PROGRAM ELEMENT NUMBER
6. AUTHOR(S)	5d. PROJECT NUMBER
	5e. TASK NUMBER
	5f. WORK UNIT NUMBER
7. PERFORMING ORGANIZATION NAME(S) AND ADDRESS(ES) **NSWC Coastal Systems Station**	8. PERFORMING ORGANIZATION REPORT NUMBER
9. SPONSORING/MONITORING AGENCY NAME(S) AND ADDRESS(ES)	10. SPONSOR/MONITOR'S ACRONYM(S)
	11. SPONSOR/MONITOR'S REPORT NUMBER(S)

12. DISTRIBUTION/AVAILABILITY STATEMENT
Approved for public release, distribution unlimited

13. SUPPLEMENTARY NOTES
See also ADM002146. Oceans 2003 MTS/IEEE Conference, held in San Diego, California on September 22-26, 2003. U.S. Government or Federal Purpose Rights License, The original document contains color images.

14. ABSTRACT

15. SUBJECT TERMS

16. SECURITY CLASSIFICATION OF:			17. LIMITATION OF ABSTRACT	18. NUMBER OF PAGES	19a. NAME OF RESPONSIBLE PERSON
a. REPORT	b. ABSTRACT	c. THIS PAGE			
unclassified	**unclassified**	**unclassified**	**UU**	**7**	

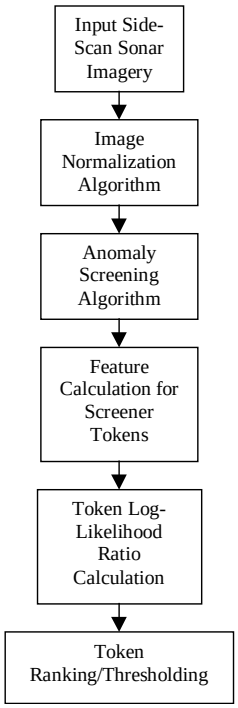

Fig. 1 Aggregate Detection/Classification Algorithm Structure

The above discussion defines the overall structure of the mine-detection/classification algorithm. Next, we describe in more detail the generic anomaly-screening algorithm depicted in Fig. 2, which is employed as a building block in the actually employed anomaly-screening algorithm. In general, an anomaly statistic is selected as some measure quantifying the deviation of behavior over some local image neighborhood, as compared to local-background characteristics. The Markov Random Field(MRF) based anomaly statistic[3] conceived in past work measured the degree of anomalousness of a specified neighborhood of pixels associated with a row in the least squares data matrix for fitting a first order MRF model. In the current image databases under investigation, ML targets have relatively small highlight regions, followed by longer shadows. Hence, in the present case a highlight/shadow contrast based anomaly statistic t_{HS} is formed as

$$t_{HS} = (mH\text{-}BNA)/(HNA\text{-}BNA) + (mS\text{-}BNA)/(SNA\text{-}BNA) \quad (1)$$

, where *mH*, *mS* denote intensity means over adjoining *ky* by *kxh*, *ky* by *kxs* windows, where *ky* denotes a pixel length in the along track direction, and (*kxh*, *kxs*) denotes pixel lengths in the range direction for highlight and shadow, respectively. The parameters *HNA*, *BNA*, *SNA* denote average highlight, background, and shadow intensities in the normalized image, respectively. Note, in addition, that kxs is allowed to vary linearly as a function of range. Given the selection of an anomaly statistic, an estimate for the anomaly statistic cumulative distribution function, *Fcda(.)* , is computed, and pixels are extracted by requiring that

$$Fcda(ta) > 1.0 - \varepsilon * .01, \quad (2)$$

where *ta* denotes the anomaly statistic value defined at a given pixel, and ε denotes the top percentage of pixels to be extracted. Next, standard computer vision[4] based region labeling algorithms are employed to obtain disconnected image Tokens or blobs. The final stages of the anomaly-screening algorithm involve the filtering of blobs to identify the most likely ML blob candidates. The maximum anomaly statistic and pixel count associated with each blob are computed and denoted by *MP*, *PC*, respectively. The associated ranks *rMP*, *rPC* are computed and the aggregate rank statistic *rMP_PC* is defined by

$$rMP\_PC = min(rMP, rPC). \quad (3)$$

Finally, the image Tokens returned by the screening algorithm are those for which

$$PCmin < PC < PCmax \quad (4)$$

$$rMP\_PC <= Thresh\_screener \quad (5)$$

,where *Thresh_screener* denotes the rank threshold required for Token selection. In the discussion that follows we will refer to the anomaly-screening algorithm as retaining the top *Thresh_screener* Tokens.

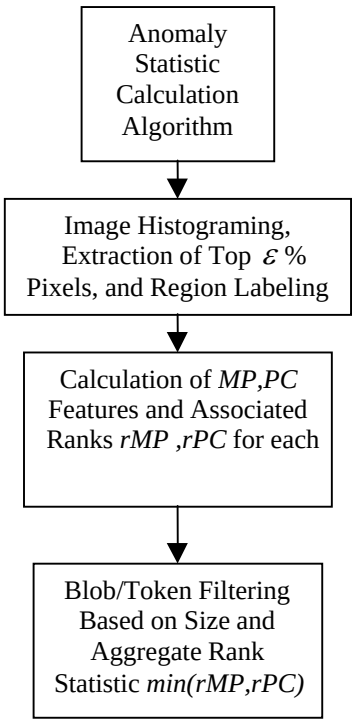

Fig. 2 Generic Anomaly-Screening Algorithm Structure

Given the above description of a generic anomaly-screening algorithm, we can define the actual screening algorithm employed. In our case, the generic anomaly screening algorithm defined above is actually applied for three distinct anomaly statistics, and the results are combined in a fashion described in the discussion that follows. We will use the notation ***A(t, b)*** to denote the anomaly-screening algorithm employing statistic t, and "filtering" parameter vector- ***b,*** where for example…

$b_1 = PCmax$ (6)
$b_2 = PCmin$
$b_3 = Thresh\_screener$
$b_4 = \varepsilon$

and the above parameters are as defined in (2), (4), and (5). In our case we make use of a highlight/shadow contrast statistic t_{HS}, as defined by (1), and an appropriate set of screening parameters- $\boldsymbol{b}_{HS}$. In addition, we make use of what will be termed "highlight", t_H, and "shadow", t_S, anomaly statistics together with associated screening parameter vectors $\boldsymbol{b}_H$, $\boldsymbol{b}_S$, respectively.

Letting $S(t, \boldsymbol{b})$ denote the image Tokens resulting from applying screening algorithm $A(t, \boldsymbol{b})$, then the aggregate screening algorithm we employ corresponds to extracting the collection of "filtered" Tokens S_F, which are the subset of $S(t_{HS}, \boldsymbol{b}_{HS})$, satisfying the below constraint for each Token T in S_F:

(T has a non-null intersection with $S(t_H, \boldsymbol{b}_H)$) or
(T has a non-null intersection with $S(t_S, \boldsymbol{b}_S)$) (7)

The motivation behind imposing the constraint in (7) is that $S(t_{HS}, \boldsymbol{b}_{HS})$-Tokens, when they correspond to genuine mine-like objects, should be associated with either a local highlight or local shadow region.

In our case, the highlight detection statistic $t_H(i,j)$ is roughly defined as

$t_H(i,j) = n(i,j)/n_M$ (8)

, where $n(i,j)$ is computed as an average of squared deviations from a local normalized image median, in the 8 directions corresponding to the nearest neighbors at a given pixel, and n_M corresponds to a median value for $n(.,.)$ in a local rectangular ring centered at (i,j). The form adopted for $t_H(i,j)$ can be motivated as a simplified form of the MRF based anomaly statistic mentioned above.

Finally, note that the adopted "shadow" detection statistic, $t_S(i,j)$, is defined as

$t_S(i,j) = -I_N(i,j)$ (9)

where $I_N(i,j)$ denotes the normalized image intensity. Hence, "shadow" blobs are derived by selecting the "tail" of the t_S distribution.

The above completes our discussion of the aggregate anomaly screening algorithm employed in the context of Figure-1. Next, we complete our discussion of the mine-hunting algorithm structure by defining the feature vector employed in the classification stage of the algorithm. In defining the calculated classification features it is important to note that three distinct segmentations are involved, corresponding to the use of the t_{HS}, t_H, t_S "anomaly" statistics, respectively, and that in addition the normalized image- I_N- is also involved. Hence, in describing the features it is necessary to denote which segmentation is involved, and the underlying image statistic employed in any calculations. The designations *HS, H, S* will be employed to denote segmentations derived from the t_{HS}, t_H, t_S "anomaly" statistics, respectively. The current baseline feature vector, f_B, is 23-dimensional and defined as follows:

f_1 = *PC for HS-segmentation* (10)
f_2 = *min(rPC, rMP) for HS-segmentation* (11)
f_3 = *"local" summation of unfiltered blob PC for HS-segmentation* (12)
f_4 = *mean t_{HS} over blob for HS-segmentation* (13)
f_5 = *standard deviation of t_{HS} over blob for HS-segmentation* (14)
f_6 = *"local" summation of unfiltered blob count for HS-segmentation* (15)
f_7 = *MP for t_{HS} over blob for HS-segmentation* (16)
f_8 = *(1,0) valued indicator for existence of intersecting H-segmentation blob* (17)
f_9 = *MP for t_H over intersecting H-segmentation blob(18)*
f_{10} = *PC for intersecting H-segmentation blob* (19)
f_{11} = *(1,0) valued indicator for existence of intersecting S-segmentation blob* (20)
f_{12} = *PC for intersecting S-segmentation blob* (21)
f_{13} = *mean I_N over blob for HS-segmentation* (22)
f_{14} = *maximum I_N over blob for HS-segmentation* (23)
f_{15} = *standard deviation of I_N over blob for HS-segmentation* (24)
f_{16} = *skewness coefficient of I_N over blob for HS-segmentation* (25)
f_{17} = *kurtosis coefficient of I_N over blob for HS-segmentation* (26)
f_{18} = *perimeter of blob for HS-segmentation* (27)
f_{19} = *(16*PC)/(perimeter*perimeter) for HS-segmentation blob* (28)
f_{20} = *perimeter/(2*(bounding-box-width + bounding-box-height)) for HS-segmentation blob* (29)
f_{21} = *(major-axis – minor-axis)/ (major-axis + minor-axis) for HS-segmentation blob* (30)
f_{22} = *major-axis* (31)
f_{23} = *orientation of HS-segmentation blob* (32)

The features *(f_6, f_3)* are defined by summations over all unfiltered blobs intersecting a 50x50 window centered at the HS-segmentation blob-centroid. The features *(f_{21}, f_{22}, f_{23})* are computed by fitting an ellipsoid to the *HS*-segmentation blob using computed "central" *x, y,* and *xy* moment information.

The above discussion defined the baseline 23 feature set, f_B. In the course of the work described here we define a Cooccurrence related feature vector, f_{COOC}, a selected subset of which is employed as input to a second MLP classifier, whose output is then employed in combination with the output of the baseline classifier, in order to obtain improved Mine Classification performance. Here, Cooccurrence matrices will be conceived as two-dimensional discrete distributions,

$p_H(i,j),\ p_V(i,j),\ p_{RD}(i,j),\ p_{LD}(i,j),$ where the subscripts *H, V, RD, LD* denote distributions associated with pairs of pixels separated by a specified number of shifts in the horizontal, vertical, right-diagonal, and left-diagonal directions, respectively. Note, that i, j denote discrete quantities assuming values $0...N_g - 1,$ obtained by quantizing some image derived from the underlying side-scan data. The calculation of a 26-dimensional Coocurrence Matrix related feature vector, denoted here by, $f_{COOC,s}$, is described as follows, where s-denotes the specified number of shifts employed in the definition of the Cooccurrence distributions:

1) Estimate cumulative histogram for window grey-levels to define N_g equal probability quantization levels
2) Calculate Empirical Cooccurrence distributions $p_H(i,j),\ p_V(i,j),\ p_{RD}(i,j),\ p_{LD}(i,j)$
3) Calculate Haralick's 13-dimensional Cooccurrence Related Feature Vector, f_{COH} with components $f_{COH,1} \ldots f_{COH,13}$, for each of the four directions, i.e. horizontal, vertical, right-diagonal, and left-diagonal.
4) Calculate feature averages over direction, $f_{ACOH,1} \ldots f_{ACOH,13}$, and the ranges of feature variation over direction, $f_{\Delta COH,1} \ldots f_{\Delta COH,13}$, in order to define an aggregate 26 dimensional feature vector, denoted by $f_{COOC,s}$.

Given the above discussion, for a sequence of shift magnitudes $s_1 \ldots s_q$, the aggregate Cooccurrence Matrix related feature vector, f_{COOC}, is defined as having partitions… $f_{cooc,s_1} \ldots f_{cooc,s_q}$. In our case we selected q=3, s_1=1, s_2=2, s_3=3. In addition, we let N_g=8, the number of bins employed in empirical cumulative histogram calculation was 15, and the image window dimension employed was 10. Finally, note that two distinct image statistics where investigated for the purpose of discretization in order to calculate Cooccurrence Matrix distributions. In each case the window was centered at the *HS*-segmentation blob centroid, but in one case**(A),** the *HS*-statistic was employed to define image intensities, while in the second case**(B),** the normalized side-scan image was employed to define image intensities.

The above serves to define the overall framework for calculation of a Cooccurrence Matrix related feature vector, f_{COOC}. The discussion that follows defines the calculation of Haralick's 13-dimensional feature vector, f_{COH}. The notation $p(i,j)$ will be employed to denote any of the directional Cooccurrence matrices mentioned above. In addition, the following notations will simplify the construction of the features:

$$p_x(i) = \sum_{j=0}^{N_g-1} p(i,j) \tag{33}$$

$$p_y(j) = \sum_{i=0}^{N_g-1} p(i,j) \tag{34}$$

$$\mu_x = \sum_{i=0}^{N_g-1} i\, p_x(i) \tag{35}$$

$$\mu_y = \sum_{j=0}^{N_g-1} j\, p_y(j) \tag{36}$$

$$\sigma_x^2 = \sum_{i=0}^{N_g-1} (i-\mu_x)^2\, p_x(i) \tag{37}$$

$$\sigma_y^2 = \sum_{j=0}^{N_g-1} (j-\mu_y)^2 p_y(j) \quad (38)$$

$$p_{x+y}(k) = \left\{ \sum_{i=0}^{k} p(i,k-i) \left[0 \le k \le N_g - 1 \right], \right. \quad (39)$$
$$\left. \sum_{i=k-N_g+1}^{N_g-1} p(i,k-i) \left[N_g - 1 \prec k \le 2(N_g-1) \right] \right\}$$

$$p_{|x-y|}(k) = \left\{ \left(\sum_{i=0}^{N_g-1} p(i,i) \right) [k=0], \right.$$
$$\left(\sum_{i=0}^{N_g-1-k} p(i,i+k) + \sum_{i=k}^{N_g-1} p(i,i-k) \right) \quad (40)$$
$$\left. [1 \le k \le N_g - 1] \right\}$$

$$HX = \sum_{i=0}^{N_g-1} -p_x(i) \ln(p_x(i)) \quad (41)$$

$$HY = \sum_{j=0}^{N_g-1} -p_y(j) \ln(p_y(j)) \quad (42)$$

$$HXY1 = \sum_{i=0}^{N_g-1} \sum_{j=0}^{N_g-1} -p(i,j) \ln(p_x(i)\, p_y(j)) \quad (43)$$

$$HXY2 = \sum_{i=0}^{N_g-1} \sum_{j=0}^{N_g-1} -p_x(i)\, p_y(j) \ln(p_x(i)\, p_y(j)) \quad (44)$$

Given the above definitions, the 13 components of Haralick's feature vector, f_{COH}, can be defined as follows:

$$f_{COH,1} = \sum_{i=0}^{N_g-1} \sum_{j=0}^{N_g-1} p(i,j) \quad (45)$$

$$f_{COH,2} = \sum_{i=0}^{N_g-1} \sum_{j=0}^{N_g-1} (i-j)^2 p(i,j) \quad (46)$$

$$f_{COH,3} = \left(\sum_{i=0}^{N_g-1} \sum_{j=0}^{N_g-1} ijp(i,j) - \mu_x \mu_y \right) / (\sigma_x \sigma_y) \quad (47)$$

$$f_{COH,4} = (\sigma_x^2 + \sigma_y^2)/2 \quad (48)$$

$$f_{COH,5} = \sum_{i=0}^{N_g-1} \sum_{j=0}^{N_g-1} p(i,j) / (1 + (i-j)^2) \quad (49)$$

$$f_{COH,6} = \sum_{i=0}^{2(N_g-1)} i\, p_{x+y}(i) \quad (50)$$

$$f_{COH,7} = \sum_{i=0}^{2(N_g-1)} (i - f_{COH,6})^2 p_{x+y}(i) \quad (51)$$

$$f_{COH,8} = \sum_{i=0}^{2(N_g-1)} -p_{x+y}(i) \ln(p_{x+y}(i)) \quad (52)$$

$$f_{COH,9} = \sum_{i=0}^{N_g-1} \sum_{j=0}^{N_g-1} -p(i,j) \ln(p(i,j)) \quad (53)$$

$$f_{COH,10} = \textit{Variance of } p_{|x-y|}(k) \textit{ distribution} \quad (54)$$

$$f_{COH,11} = \sum_{k=0}^{N_g-1} -p_{|x-y|}(k) \ln(p_{|x-y|}(k)) \quad (55)$$

$$f_{COH,12} = (f_{COH,9} - HXY1) / \max(HX, HY) \quad (56)$$

$$f_{COH,13} = (1 - \exp(-2(HXY2 - f_{COH,9})))^{.5} \quad (57)$$

III.COMPARISON OF TEXTURE MEASURE AUGMENTED, AND BASELINE CLASSIFIER PERFORMANCE RESULTS

Recall in the above discussion that two cases, designated **(A)**, **(B)** are defined corresponding to the use of HS-statistic data, and normalized side-scan image data, respectively, in constructing the aggregate 78-dimensional Cooccurrence related feature vector, denoted by f_{COOC}. In each case, the Genetic Algorithm based approach to feature selection embedded in Neuralware's state of the art Cascade Correlation Network Classification model builder is employed to select 18, and 10 features for cases **(A)**, **(B),** respectively.

In Fig.-3 the Baseline 23F classification performance is compared with the 18F and 10F performance, respectively. Note, that FAI denotes the average number of false alarms per image, and PCD denotes the cumulative Mine classification probability, over a test data set of 244 images. This test data set is distinct from the 56 images employed for training. In addition, in Fig.-3 upper and lower 90% coverage probability confidence bounds for the 23F baseline performance are displayed, as obtained using the Boostrap Based approach detailed in [5]. These results demonstrate that the 10F, 18F cases have classification performance that is significantly worse, in a statistical sense, than the 23F baseline case.

In order to investigate the performance achievable by the fusion of the baseline 23F and either of Cooccurrence Matrix Feature cases **(A)**, **(B),** we consider the selection of joint/simultaneous classification thresholds associated with the output of a 23F classifier, and a Cooccurrence Matrix Feature related classifier, respectively, in order to minimize the achieved number of false alarms, at each specified number of classified targets. In Fig. 4 and 5 we present the (FAI, PCD) curves associated with the fused (23F, 18F) and (23F, 10F), cases respectively, together with the baseline 23F performance. In addition, in each case we present upper and lower, 90% coverage bounds associated with the fused performance. In this case however, the resulting Bootstrap derived bounds are *conditioned on a specified range of classified targets being achievable, based on appropriate joint threshold selections associated with the outputs of individual classifiers.* Hence, this is equivalent to conditioning on a fixed collection of PCD values being achievable, and determining upper and lower bounds on the achievable FAI performance.

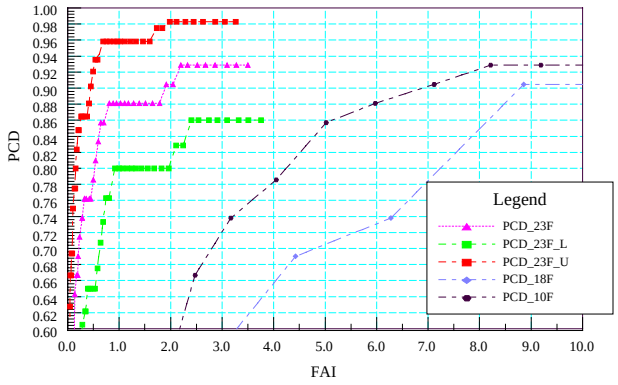

Fig.-3 Comparison of Classification Performance for Baseline 23F and Cooccurrence Matrix Feature Derived Cases **(A)**, **(B),** respectively

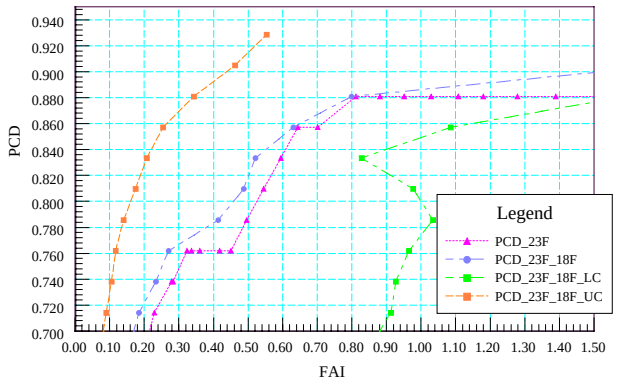

Fig.-4 Comparison of Classification Performance for Baseline 23F and Fused (23F,18F) Cases, Respectively

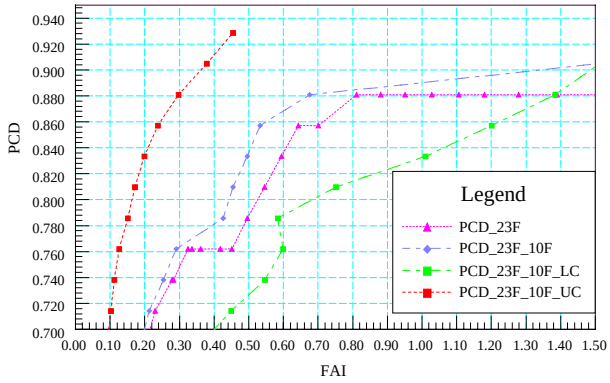

Fig.-5 Comparison of Classification Performance for Baseline 23F and Fused (23F,10F) Cases, Respectively

IV.CONCLUSIONS

Results in Fig. 3-5 demonstrate that while the Cooccurrence related features computed from the normalized side-scan image are more powerful for mine/clutter discrimination, than those computed from the HS-segmentation statistic, the fusing of either set of features with the Baseline 23F set does not result in statistically significant performance improvement, relative to the Baseline case.

ACKNOWLEDGEMENTS

This work was funded by the Office of Naval Research(ONR 321OE, ONR 32MIW) as part of the Mine Countermeasures Program(FNC). The technical agent for this work was NSWC, Coastal Systems Station(CSS), Dahlgren Division.

REFERENCES

1. Haralick, R.M. et. al., “Textural Features for Image Classification”, *IEEE Transactions on Systems, Man, and Cybernetics*, V. SMC-3, No. 6, November 1973,pp. 610-621.
2. D.H.Kill et. al., “Reducing Model- and Data-Mismatch Errors in Image Compression by Combining Region Dependent Transform-Coefficient Encoding with Normalization and Content-Adaptive Coding”, (submitted for publication to the *IEEE Journal of Ocean Engineering*).
3. M.G. Bello, "A Markov Random Field Based Anomaly Screening Algorithm", *Proceeding of SPIE '95*,Vol. 2496, April 1995.
4. R Haralick and L. Shapiro, *Computer and Robot Vision Volume-I*, Addison Wesley Publishing Co., Reading, Mass.,1992.
5. M. G. Bello, “Comparison of Parametric and Nonparametric ROC Confidence Bound Construction in the Context of Acoustic/Magnetic Fusion Systems for Mine Hunting”, *Proceedings of SPIE’98*, Orlando, Florida, April 1998.